DOI 10.59887/2073-6673.2023.16(4)-9

UDC 551.46.08

© *V. A. Glukhov**[1], *Yu. A. Goldin*[1], *O. V. Glitko*[1], *E. A. Aglova*[1,2], *D. I. Glukhovets*[1,2], *M. A. Rodionov*[1], 2023

© Translation from Russian: *E. A. Aglova, V. A. Glukhov*, 2023

[1]Shirshov Institute of Oceanology, Russian Academy of Sciences, 36 Nakhimovsky Prosp., Moscow 117997, Russia
[2]Moscow Institute of Physics and Technology (National Research University), 9 Institutskiy per., Dolgoprudny, Moscow region, 141701, Russia
*vl.glukhov@inbox.ru

LIDAR RESEARCH DURING THE FIRST STAGE OF THE 89th CRUISE OF THE R/V 'ACADEMIC MSTISLAV KELDYSH'

Received 05.10.2023, Revised 04.12.2023, Accepted 06.12.2023

Abstract

A lidar survey of the western part of the Kara Sea was carried out in September 2022. The shipborne radiometric (profiling) lidar PLD-1 was used. The lidar optical unit was located on the 8th deck of the R/V 'Akademik Mstislav Keldysh' at an altitude of 15 m above the water surface. Lidar sounding was carried out at stations and underway. The vessel route passed through water areas characterized by a wide range of changes in hydrooptical characteristics. Lidar measurements were accompanied by synchronized measurements of hydrooptical and hydrological characteristics. These measurements were carried out using submersible instruments at stations and using a flow-through measuring complex along the ship's route. The hydrooptical characteristics vertical distribution uniformity in the upper ten-meter layer was controlled remotely using underway lidar data. Good agreement between the spatial distributions of the lidar echo signals parameters, of the hydrooptical and of the hydrological characteristics (coincidence of the locations of various distribution features, local maxima, minima and frontal zones) was demonstrated. A large volume of measurement data has been obtained, which allows for further statistical processing in order to find relationships between the parameters of lidar echo signals and hydrooptical characteristics recorded by contact methods.

Keywords: marine lidar, hydrooptical characteristics, lidar survey, frontal zones, Kara Sea

УДК 551.46.08

© *В. А. Глухов*[1]*, *Ю. А. Гольдин*[1], *О. В. Глитко*[1], *Е. А. Аглова*[1,2], *Д. И. Глуховец*[1,2], *М. А. Родионов*[1], 2023

© Перевод с русского: *Е. А. Аглова*, *В. А. Глухов*, 2023

[1]Институт океанологии им. П.П. Ширшова РАН, 117997, Москва, Нахимовский пр-т, д. 36
[2]Московский физико-технический институт (национальный исследовательский университет), 141701, Институтский пер., д. 9, г. Долгопрудный, Московская область, Россия
*vl.glukhov@inbox.ru

ЛИДАРНЫЕ ИССЛЕДОВАНИЯ В ПЕРВОМ ЭТАПЕ 89-ГО РЕЙСА НИС «АКАДЕМИК МСТИСЛАВ КЕЛДЫШ»

Статья поступила в редакцию 05.10.2023, после доработки 04.12.2023, принята в печать 06.12.2023

Аннотация

Выполнена лидарная съемка западной части Карского моря. Съемка проводилась в сентябре 2022 г. Использован судовой радиометрический (профилирующий) лидар ПЛД-1. Оптический блок лидара располагался на 8-й палубе НИС «Академик Мстислав Келдыш» на высоте 15 м над поверхностью воды. Лидарное зондирование проводилось на станциях и на ходу судна. Маршрут судна проходил через акватории, характеризующиеся широким диапазоном изменений гидрооптических характеристик. Лидарные измерения сопровождались комплексом сопутствующих измерений гидрооптических и гидрологических характеристик. Сопутствующие измерения выполнялись на станциях с использованием погружаемых приборов, а также на ходу судна с помощью проточного измерительного комплекса. Однородность вертикального распределения гидрооптических характеристик

Ссылка для цитирования: *Глухов В.А.*, *Гольдин Ю.А.*, *Глитко О.В.*, *Аглова Е.А.*, *Глуховец Д.И.*, *Родионов М.А.* Лидарные исследования в первом этапе 89-го рейса НИС «Академик Мстислав Келдыш» // Фундаментальная и прикладная гидрофизика. 2023. Т. 16, № 4. С. 107–115. doi:10.59887/2073-6673.2023.16(4)-9
For citation: *Glukhov V.A.*, *Goldin Yu.A.*, *Glitko O.V.*, *Aglova E.A.*, *Glukhovets D.I.*, *Rodionov M.A.* Lidar Research during the First Stage of the 89th Cruise of the R/V 'Academic Mstislav Keldysh'. *Fundamental and Applied Hydrophysics*. 2023, 16, 4, 107–115. doi:10.59887/2073-6673.2023.16(4)-9

на ходу судна в верхнем десятиметровом слое контролировалась дистанционным методом по лидарным данным. Продемонстрировано хорошее согласие пространственных распределений параметров лидарных эхо-сигналов, гидрооптических и гидрологических характеристик (совпадение пространственных положений различных особенностей распределения, локальных максимумов, минимумов и фронтальных зон). Получен большой объем данных измерений, позволяющих в дальнейшем провести их статистическую обработку с целью нахождения связей между параметрами лидарных эхо-сигналов и гидрооптическими характеристиками, зарегистрированными контактными методами.

Ключевые слова: морской лидар, гидрооптические характеристики, лидарная съемка, фронтальные зоны, Карское море

1. Introduction

The lidar remote sensing capabilities for study of seawater near-surface layers have been demonstrated in a number of works [1–5]. The advantage of using shipborne and airborne marine lidars is the remote registration of the near-surface layer hydrooptical characteristics [5–8]. In order to obtain hydrooptical characteristics from radiometric lidar data, we usually assume the vertical distribution of the studied layer is uniform. In recent years, researchers have developed methods to determine the vertical distributions of hydrooptical characteristics even in the presence of stratification. For this purpose, high spectral resolution lidars (HSRL) are used, which combine registration of the temporal and spectral dependences of the echo signal [9, 10].

The methods used to obtain information about hydrooptical characteristics from lidar data depend on the specific lidar characteristics and the sensing geometry in each case [7, 11]. There is no universal algorithm for recalculating the parameters of registered lidar echo signals. This necessitates the need to carry out measurements with specific lidars in certain water areas. A corresponding region for conducting such studies is the Kara Sea, which is characterized by high spatial variability of hydrooptical characteristics in a wide range of their values [12–14]. The advantage of shipborne lidar survey is the ability to carry out underway without the use of submersible devices, as well as the capability to carry out synchronous accompanying measurements of hydrooptical and hydrological characteristics.

This paper presents the results of lidar measurements conducted both at stations and along the ship's route. The study compares the spatial distributions of lidar echo signal parameters with the corresponding distributions of hydrooptical and hydrological characteristics obtained during synchronous accompanying measurements.

2. Materials and methods

2.1. Description of the equipment

The shipborne polarization lidar PLD-1 (developed at the Shirshov Institute of Oceanology RAS [15]) was used to carry out the research. Its operating wavelength is 532 nm, the probing pulse duration is 7 ns (FWHM), the energy of the probing pulse is 20 mJ, the field of view angle of the receiving optical system is 0.9 degrees (15.5 mrad), input lens diameter is 63 mm. A LeCroy HDO4034 digital four-channel oscilloscope was used to digitize and record lidar echo signals. The sampling rate is 2.5 GHz, the dynamic range is 14 bits. The PLD-1 has two receiving channels designed for recording co- and cross-polarized components of the lidar echo signal. In this paper only the co-polarized components of the lidar echo signal are analyzed.

The lidar optical unit was placed on the 8th deck of the R/V 'Akademik Mstislav Keldysh'. The optical unit altitude is about 15 m above the water surface. Sensing angle $\theta = 20°$ from the vertical. The air section length of the sounding path H was about 16 meters. Simultaneously with the registration of lidar echo signals, navigation position data were recorded using signals from the GLONASS/GPS satellite navigation systems.

Lidar echo signals were recorded with a frequency of 1 Hz during the cruise. Measurements were carried out both during the stations and underway. At a ship speed of 10 knots, the measurement points were spatially discrete at approximately 5 meters apart.

In addition to the lidar survey, a series of synchronized accompanying measurements were carried out. At the stations measurements of vertical profiles of the seawater beam attenuation coefficient c were carried out at a wavelength $\lambda = 530$ nm using a submersible transmissometer PUM-200 (developed at the Shirshov Institute of Oceanology RAS [16, 17]). The measurement accuracy of c is in the range of 0.050–1.0 m^{-1} is 0.005 m^{-1}.

As the seawater beam attenuation coefficient increases above 1 m^{-1}, the influence of multiple scattering increases, which leads to an increase in the measurement error. The assessment of the variability of the seawater beam attenuation coefficient in this range is qualitative.

Using the shipboard flow-through measuring complex (Shirshov Institute of Oceanology RAS), continuous measurements were carried out along the ship route [18]. The complex allows to measure seawater temperature T and specific electrical conductivity, which is then converted into salinity S. The four-channel spectral flow-through fluorimeter included in the complex makes it possible to determine the fluorescence intensity of colored dissolved organic matter (CDOM) — I_{CDOM}, induced by laser radiation with an excitation wavelength of 405 nm. Fluorescence intensity values are converted to Raman units (R.U.) by normalizing the fluorescence peak to the Raman peak of water molecules. The complex also includes a universal transmissometer PUM-A for determining the seawater beam attenuation coefficient c values at a wavelength of 530 nm. The technical characteristics of PUM-A are similar to those of PUM-200 given above. The water intake depth is 2–3 m. The spatial resolution of the data is about 50 m. The measured data were referenced using signals from the GPS satellite navigation system.

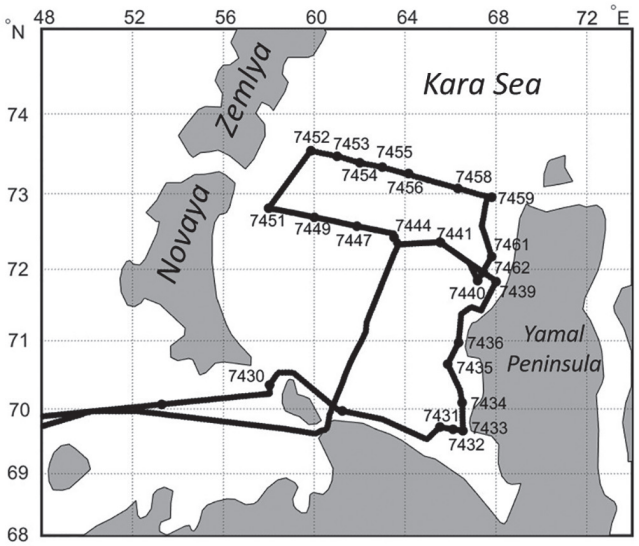

Fig. 1. The vessel route and the station positions of the 1st stage of the 89th cruise of the R/V 'Akademik Mstislav Keldysh' in the Kara Sea

2.2. Research area

The work was carried out as part of the 1st stage of the 89th cruise of the R/V 'Akademik Mstislav Keldysh' in the western part of the Kara Sea from September 5 to 19, 2022. The vessel route and station positions are shown in Figure 1.

2.3. Lidar data processing method

Following the lidar equation, the lidar attenuation coefficient $\alpha(z)$ describes the exponential weakening of the echo signal [1]:

$$P\left(t=\frac{2Z}{c_w}\right)=P_0\frac{AT_O(1-r)^2}{(nH+Z)^2}\beta(\pi,Z)\exp\left[-2\int_0^Z\alpha(Z')dZ'\right], \quad (1)$$

where Z and H are the lengths of the underwater and above-water sections of the sounding path, c_w is the speed of light in sea water, n is the refractive index of sea water, $\alpha(Z)$ is the attenuation index of the lidar echo signal, $\beta(\pi, Z)$ is the vertical profile of the volum scattering function taken at the scattering angle 180°, P_0 the power of an initial laser pulse, A is the size of the receiving aperture, T_O is the transmittance of the receiving system, $r \approx 0.02$ is the Fresnel reflection coefficient. The true depth z can be calculated from Z taking into account the sounding angle θ.

In general, it depends on the vertical distribution of near-surface layer hydrooptical characteristics. Depending on the profiling geometry, the α values vary from K_d to c; this means the K_d value corresponding to the position of the sun at the zenith and if there were no atmosphere [11]. In the case of uniform waters, α is a constant value. To determine α, a standard approach based on the use of lidar echo signal approximations by a function, which form follows from the lidar equation, was used [5, 19]. The echo signal section corresponding to a depth range from 4 to 8 m was used for determining α. The layer above 4 m is subject to strong influence of surface waves. In many cases, variability in hydrooptical characteristics is observed at depths below 8–10 m.

Examples of co-polarized lidar echo signals and corresponding approximating functions are shown in Figure 2. All measurements were carried out in the linear mode of the PMT. To prevent saturation, the high-voltage supply of the PMT was adjusted. Figures 2, *a* and *b* show waters of varying transparency, uniform in depth in a layer from the surface to 10 m. Figure 2, *a* illustrates the case of the high transparency waters in which the single scattering model works and the lidar attenuation coefficient α is close to the seawater beam attenuation coefficient *c*. Figure 2, *b* illustrates the case of the high value of the scattering coefficient in which the effective radiation pattern of the receiver becomes wide and α is close to the diffuse attenuation coefficient K_d.

The variance value of the seawater beam attenuation coefficient was used as a criterion for the vertical distribution homogeneity in a layer from 0 to 10 m. At the station 7453 (Figure 2, *a*) the dispersion value of *c* was $6 \cdot 10^{-6}$ m^{-2}, at the station 7433 (Figure 2, *b*) it was $5 \cdot 10^{-6}$ m^{-2}. Figure 2, *c* shows the lidar echo signal corresponding to the inhomogeneous layer at a depth of 0 to 10 m. The variance value of c at this station was $2 \cdot 10^{-3}$ m^{-2}. In this case the lidar echo signal has a more complex form. It requires the use of several approximations to describe it. In this regard, for further analysis only those stations were used where layer at a depth of 0 to 10 m was homogeneous in terms of a variance value of less than 10^{-5} m^{-2}.

When processing lidar survey data, the α value for each recorded lidar echo signal was determined. At stations, which duration ranged from 1 to 3 hours, all obtained values of α were averaged (from 3 to 11 thousand soundings), which made it possible to reduce the influence of random measurement errors. The constancy of the hydrooptical characteristics at the stations was monitored by the form of the lidar echo signal and the absence of significant variability in α over time. Measurement data obtained underway were averaged over the results of 100 soundings (spatial averaging interval was about 500 m) to reduce the influence of the vessel pitching, waves and foam.

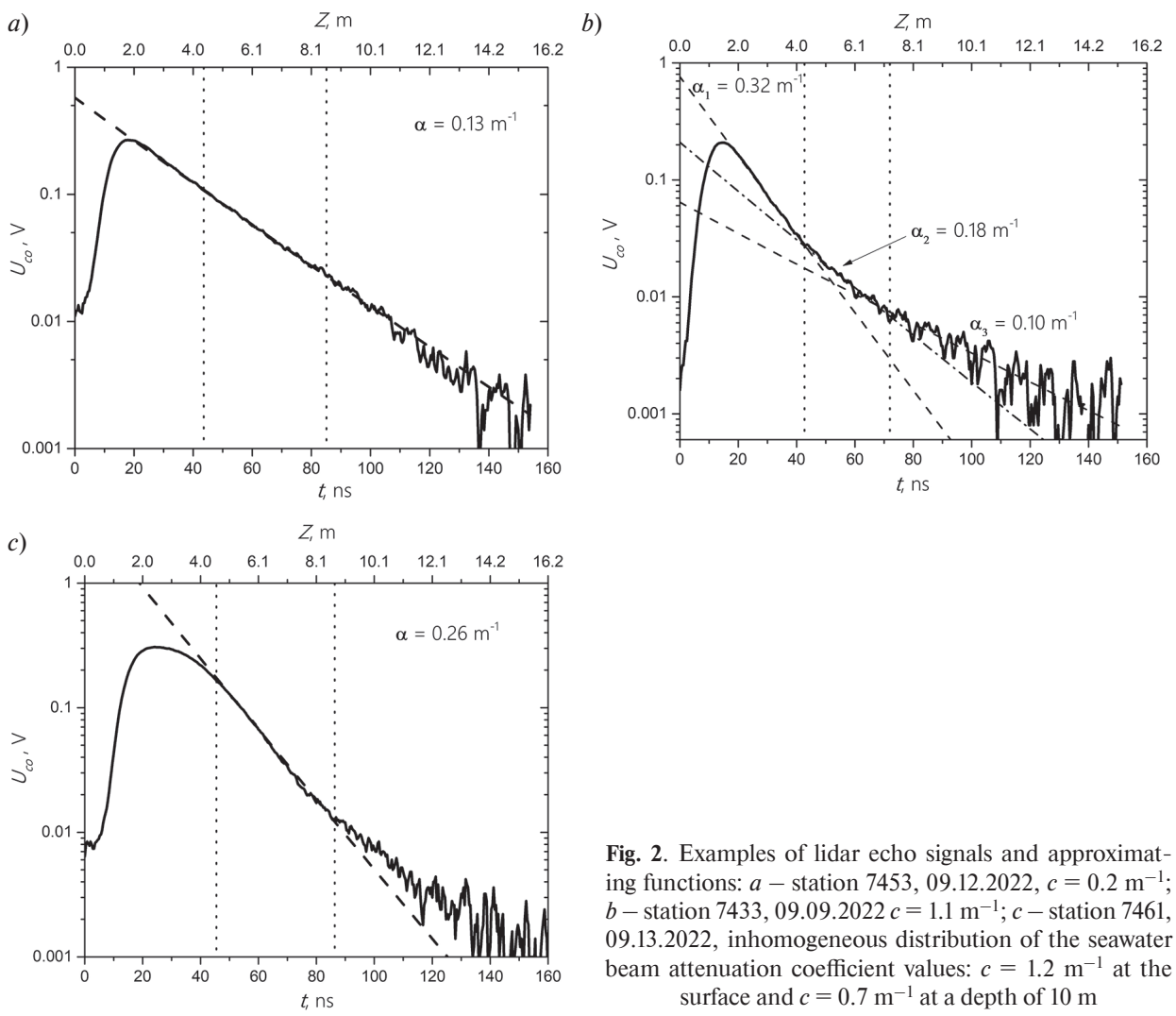

Fig. 2. Examples of lidar echo signals and approximating functions: *a* – station 7453, 09.12.2022, $c = 0.2$ m^{-1}; *b* – station 7433, 09.09.2022 $c = 1.1$ m^{-1}; *c* – station 7461, 09.13.2022, inhomogeneous distribution of the seawater beam attenuation coefficient values: $c = 1.2$ m^{-1} at the surface and $c = 0.7$ m^{-1} at a depth of 10 m

3. Results and discussion

The lidar survey was carried out both at stations and along the vessel route for about 270 hours. A uniform depth distribution of the seawater beam attenuation coefficient c in the upper layer at depths from the surface up to 10 m at 27 stations on different sections of the route was recorded. For each of these stations, the average value of the lidar attenuation coefficient α and the standard deviation of the measured value were calculated. The distributions of α and *c* values measured at stations along the vessel route are presented in Figure 3. The measurement range of *c* was from 0.17 m^{-1} to 1.1 m^{-1}. There are a good agreement in the type of distributions and coincidences in the position of distribution features, local maxima, minima and frontal zones. The resulting set of pairs of values α and c makes it possible to further carry out their statistical analysis to establish regression relationships. The given distribution α contains information about the spatial distribution of hydrooptical characteristics and can be successfully used to carry out remote measurements of these characteristics using the lidar method.

An example of the measurement results carried out underway is shown in Figure 4. This figure depicts the section of the track from the Kara Gate Strait to Baydaratskaya Bay, conducted on September 8, 2022, between the stations 7430 and 7431. Comparison of the spatial distributions of α and *c*, measured by the flow-through complex along the vessel route are shown in Figure 4, *a*. The corresponding distributions of salinity *S*, temperature *T* and CDOM fluorescence intensity I_{CDOM}, also measured with the flow-through complex, are shown in Figure 4, *b*. The type of variability of α is in good agreement with the type of other distributions variability. The distribution of the lidar attenuation coefficient α effectively determines the position of the fronts. It should be noted the section shows a negative correlation between the distributions of *S* and I_{CDOM}. This indicates the section is located in the zone of influence of the river runoff [12, 13].

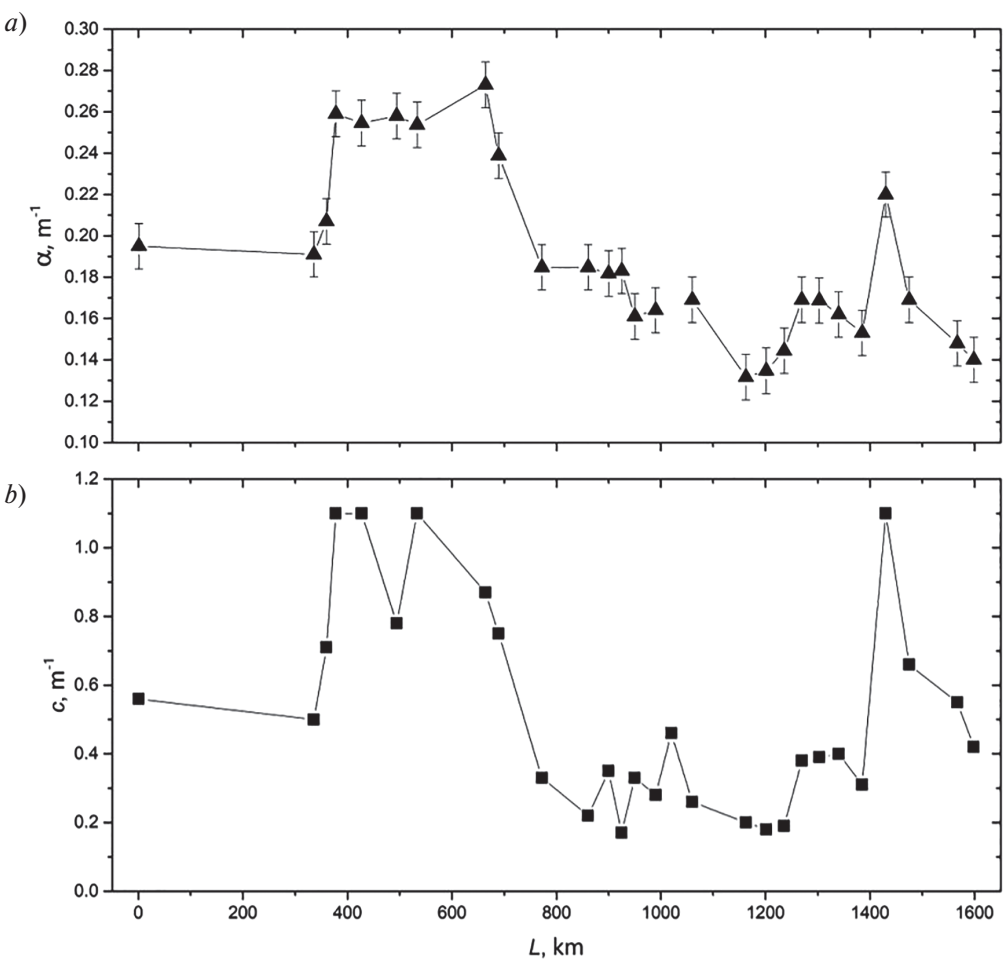

Fig. 3. Distributions of α and *c* values measured at stations along the vessel's route

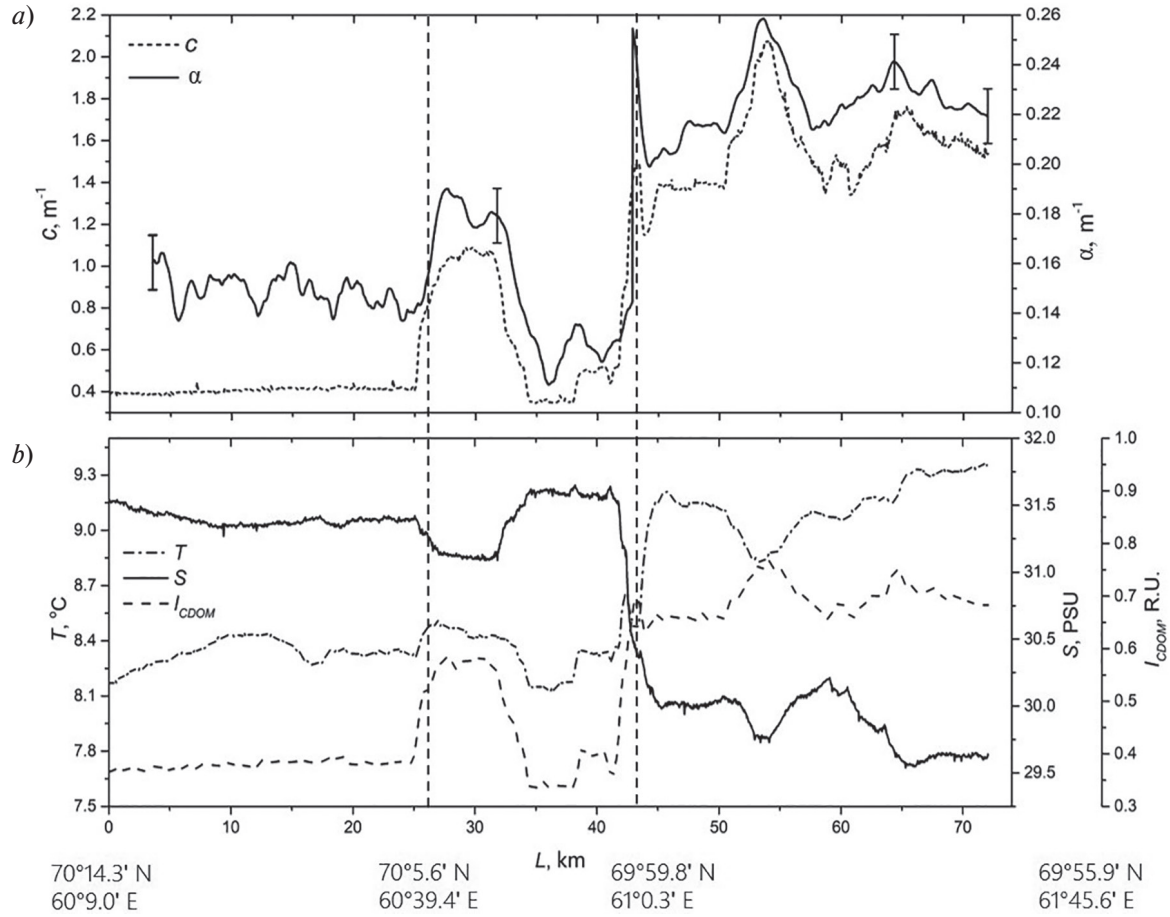

Fig. 4. Cross-section along the ship route, carried out on the section between the stations 7430 and 7431: a — α and c, b — T, S, I_{CDOM}

4. Conclusion

A lidar survey of the western part of the Kara Sea was conducted using shipborne polarization lidar PLD-1. Analysis of the obtained data showed a high similarity in the distributions of the lidar attenuation coefficient α and the seawater beam attenuation coefficient c. The spatial distributions of α, c, temperature, salinity, and CDOM fluorescence intensity were compared. A good agreement between the parameters of the obtained distributions and the coincidence of the locations of various distribution features, local maxima, minima and frontal zones has been demonstrated.

A large array of lidar sounding data and synchronous accompanying measurements was obtained. This makes it possible to carry on further statistical analysis and establishment of regression relationships between hydrooptical characteristics and parameters of lidar echo signals. The presence of such relationships will give the opportunity to carry out quantitative measurements of hydrooptical characteristics by the lidar method using the PLD-1 lidar. As we continue our work, it will be of interest to analyze the cross-polarized lidar echo signal, which is formed mainly by multiply scattering.

Acknowledgments

The authors gratefully acknowledge V.A. Artemyev for assistance in carrying out contact measurements.

Funding

Processing and analysis of the lidar data array were carried out as a part of the state assignment of Shirshov Institute of Oceanology No. FMWE-2021-0014. Acquisition and processing of contact measurements data were carried out with the financial support of the Russian Science Foundation (project No. 21-77-10059).

References

1. *Vasilkov A.P.*, *Goldin Yu.A.*, *Gureev B.A.* et al. Airborne polarized lidar detection of scattering layers in the ocean. *Applied Optics*. 2001, 40, 4353–4364. doi:10.1364/AO.40.004353
2. *Churnside J.H.*, *Donaghay P.L.* Thin scattering layers observed by airborne lidar. *ICES Journal of Marine Science*. 2009, 66(4), 778–789. doi:10.1093/icesjms/fsp029
3. *Churnside J.H.*, *Ostrovsky L.A.* Lidar observation of a strongly nonlinear internal wave train in the Gulf of Alaska. *International Journal of Remote Sensing*. 2005, 26(1), 167–177. doi:10.1080/01431160410001735076
4. *Churnside J.H.*, *Brown E.D.*, *Parker-Stetter S.* et al. Airborne remote sensing of a biological hot spot in the southeastern Bering Sea. *Remote Sensing*. 2011, 3(3), 621–637. doi:10.3390/rs3030621
5. *Collister B.L.*, *Zimmerman R.C.*, *Hill V.J.*, *Sukenik C.I.*, *Balch W.M.* Polarized lidar and ocean particles: insights from a mesoscale coccolithophore bloom. *Applied Optics*. 2020, 59(15), 4650–4662. doi:10.1364/AO.389845
6. *Goldin Y.A.*, *Vasilev A.N.*, *Lisovskiy A.S.*, *Chernook V.I.* Results of Barents Sea airborne lidar survey. *Current Research on Remote Sensing, Laser Probing, and Imagery in Natural Waters. SPIE*. 2007, 6615, 126–136. doi:10.1117/12.740456
7. *Xu P.*, *Liu D.*, *Shen Y.* et al. Design and validation of a shipborne multiple-field-of-view lidar for upper ocean remote sensing. *Journal of Quantitative Spectroscopy and Radiative Transfer*. 2020, 254, 107201. doi:10.1016/j.jqsrt.2020.107201
8. *Kokhanenko G.P.*, *Balin Y.S.*, *Penner I.E.*, *Shamanaev V.S.* Lidar and *in situ* sensing of the upper layers of Baikal Lake water. *Atmospheric and Oceanic Optics*. 2011, 24(5), 478–486. doi:10.1134/S1024856011050083
9. *Schulien J.A.*, *Behrenfeld M.J.*, *Hair J.W.* et al. Vertically-resolved phytoplankton carbon and net primary production from a high spectral resolution lidar. *Optics Express*. 2017, 25, 13577–13587. doi:10.1364/OE.25.013577
10. *Zhou Y.*, *Chen Y.*, *Zhao H.* et al. Shipborne oceanic high-spectral-resolution lidar for accurate estimation of seawater depth-resolved optical properties. *Light: Science & Applications*. 2022, 11(261). doi:10.1038/s41377-022-00951-0
11. *Gordon H.R.* Interpretation of airborne oceanic lidar: effects of multiple scattering. *Applied Optics*. 1982, 21(16), 2996–3001. doi:10.1364/AO.21.002996
12. *Burenkov, V.I.*, *Goldin, Y.A.*, *Artem'ev, V.A.* et al. Optical characteristics of the Kara Sea derived from shipborne and satellite data. *Oceanology,* 2010, 50, 675–687. doi:10.1134/S000143701005005X
13. *Burenkov V.I.*, *Goldin Yu.A.*, *Gureev B.A.*, *Sudbin A.I.* Basic ideas about the distribution of optical properties of the Kara Sea. *Oceanology*. 1995, 35(3), 376–387 (in Russian).
14. *Konik A.A.*, *Zimin A.V.*, *Atadzhanova O.A.* Spatial and temporal variability of the characteristics of the river plume frontal zone in the Kara Sea in the first two decades of the XXI century. *Fundamental and Applied Hydrophysics*. 2022, 15(4), 23–41. doi:10.59887/fpg/38mu-zda7-dpep
15. *Glukhov V.A.*, *Goldin Yu.A.*, *Rodionov M.A.* Experimental estimation of the capabilities of the lidar PLD-1 for the registration of various hydro-optical irregularities of the sea water column. *Fundamental and Applied Hydrophysics*. 2017, 10(2), 41–48. doi:10.7868/S207366731702006X (in Russian).
16. *Burenkov V.I.*, *Sheberstov S.V.*, *Artemiev V.A.*, *Taskaev V.R.* Estimation of measurement error of the seawater beam attenuation coefficient in turbid water of Arctic seas. *Light & Engineering*. 2019, 2, 55–60. doi:10.33383/2018–100
17. *Artemyev V.A.*, *Taskaev V.R.*, *Grigoriev A.V.* Autonomous transparent meter PUM-200. *Materials of the XVII international scientific and technical conference: Modern methods and means of oceanological research (MSOI-2021). P.P. Shirshov Institute of Oceanology RAS. Moscow*. 2021, 95–99 (in Russian).
18. *Goldin Y.A.*, *Glukhovets D.I.*, *Gureev B.A.* et al. Shipboard flow-through complex for measuring bio-optical and hydrological seawater characteristics. *Oceanology*. 2020, 60, 713–720. doi:10.1134/S0001437020040104
19. *Glukhov V.A., Goldin Yu.A.*, *Rodionov M.A.* Method of internal waves registration by lidar sounding in case of waters with two-layer sratification of hydrooptical characteristics. *Fundamental and Applied Hydrophysics*. 2021, 14(3), 86–97. doi:10.7868/S2073667321030084 (In Russian).

Литература

1. *Vasilkov A.P.*, *Goldin Yu.A.*, *Gureev B.A.* et al. Airborne polarized lidar detection of scattering layers in the ocean // Applied Optics. 2001. Vol. 40, N 24. P. 4353–4364. doi:10.1364/AO.40.004353
2. *Churnside J.H.*, *Donaghay P.L.* Thin scattering layers observed by airborne lidar // ICES Journal of Marine Science. 2009. Vol. 66, N 4. P. 778–789. doi:10.1093/icesjms/fsp029
3. *Churnside J.H.*, *Ostrovsky L.A.* Lidar observation of a strongly nonlinear internal wave train in the Gulf of Alaska // International Journal of Remote Sensing. 2005. Vol. 26, N 1. P. 167–177. doi:10.1080/01431160410001735076
4. *Churnside J.H.*, *Brown E.D.*, *Parker-Stetter S.* et al. Airborne remote sensing of a biological hot spot in the southeastern Bering Sea // Remote Sensing. 2011. Vol. 3, N 3. P. 621–637. doi:10.3390/rs3030621
5. *Collister B.L.*, *Zimmerman R.C.*, *Hill V.J.*, *Sukenik C.I.*, *Balch W.M.* Polarized lidar and ocean particles: insights from a mesoscale coccolithophore bloom // Applied Optics. 2020. Vol. 59, N 15. P. 4650–4662. doi:10.1364/AO.389845
6. *Goldin Y.A.*, *Vasilev A.N., Lisovskiy A.S.*, *Chernook V.I.* Results of Barents Sea airborne lidar survey // Current Research on Remote Sensing, Laser Probing, and Imagery in Natural Waters SPIE. 2007. Vol. 6615. P. 126–136.
   doi:10.1117/12.740456
7. *Xu P.*, *Liu D.*, *Shen Y.* et al. Design and validation of a shipborne multiple-field-of-view lidar for upper ocean remote sensing // Journal of Quantitative Spectroscopy and Radiative Transfer. 2020. Vol. 254. P. 107201.
   doi:10.1016/j.jqsrt.2020.107201
8. *Коханенко Г.П.*, *Балин Ю.С.*, *Пеннер И.Э.*, *Шаманаев В.С.* Лидарные и in situ измерения оптических параметров поверхностных слоев воды в озере Байкал // Оптика атмосферы и океана. 2011. Т. 24, № 5. С. 377–385.
9. *Schulien J.A.*, *Behrenfeld M.J.*, *Hair J.W.* et al. Vertically- resolved phytoplankton carbon and net primary production from a high spectral resolution lidar // Optics Express. 2017. Vol. 25. P. 13577–13587. doi:10.1364/OE.25.013577
10. *Zhou Y.*, *Chen Y.*, *Zhao H.* et al. Shipborne oceanic high-spectral-resolution lidar for accurate estimation of seawater depth-resolved optical properties // Light: Science & Applications. 2022. Vol. 11, N 261. doi:10.1038/s41377-022-00951-0
11. *Gordon H.R.* Interpretation of airborne oceanic lidar: effects of multiple scattering // Applied Optics. 1982. Vol. 21, N 16. P. 2996–3001. doi:10.1364/AO.21.002996
12. *Буренков В.И.*, *Гольдин Ю.А.*, *Артемьев В.А.*, *Шеберстов С.В.* Оптические характеристики вод Карского моря по судовым и спутниковым наблюдениям // Океанология. 2010. Т. 50, № 5. С. 716–729. doi:10.1134/S000143701005005X
13. *Буренков В.И.*, *Гольдин Ю.А.*, *Гуреев Б.А.*, *Судьбин А.И.* Основные представления о распределении оптических свойств Карского моря // Океанология. 1995. Т. 35, № 3. С. 376–387.
14. *Коник А.А.*, *Зимин А.В.*, *Атаджанова О.А.* Пространственно-временная изменчивость характеристик стоковой фронтальной зоны в Карском море в первые два десятилетия XXI века // Фундаментальная и прикладная гидрофизика. 2022. Т. 15, № 4. С. 23–41. doi:10.59887/fpg/38mu-zda7-dpep
15. *Глухов В.А.*, *Гольдин Ю.А.*, *Родионов М.А.* Экспериментальная оценка возможностей лидара ПЛД-1 по регистрации гидрооптических неоднородностей в толще морской среды // Фундаментальная и прикладная гидрофизика. 2017. Т. 10, № 2. С. 41–48. doi:10.7868/S207366731702006X
16. *Буренков В.И.*, *Шеберстов С.В.*, *Артемьев В.А.*, *Таскаев В.Р.* Оценка погрешности измерения показателя ослабления света морской водой в мутных водах арктических морей // Светотехника. 2019. Т. 2. С. 55–60. doi:10.33383/2018-100
17. *Артемьев В.А.*, *Таскаев В.Р.*, *Григорьев А.В.* Автономный прозрачномер ПУМ-200 // Современные методы и средства океанологических исследований (МСОИ-2021). Материалы XVII международной научно-технической конференции. Институт океанологии им. П.П. Ширшова РАН. 2021. С. 95–99.
18. *Гольдин Ю.А.*, *Глуховец Д.И.*, *Гуреев Б.А.* и др. Судовой проточный комплекс для измерения биооптических и гидрологических характеристик морской воды // Океанология. 2020. Т. 60, № 5. С. 814–822.
   doi:10.31857/S0030157420040103
19. *Глухов В.А.*, *Гольдин Ю.А.*, *Родионов М.А.* Лидарный метод регистрации внутренних волн в водах с двухслойной стратификацией гидрооптических характеристик // Фундаментальная и прикладная гидрофизика. 2021. Т. 14, № 3. С. 86–97. doi:10.7868/S2073667321030084

About the Authors

GLUKHOV, Vladimir A., РИНЦ AuthorID: 916467, ORCID ID: 0000-0003-4555-8879, Scopus AuthorID: 57191414331, WoS ResearcherID: GSD-4886-2022, vl.glukhov@inbox.ru

GOLDIN, Yuriy A., Cand.Sc. (Phys.-Math.), РИНЦ AuthorID: 58653, ORCID ID: 0000-0001-5731-5458, Scopus AuthorID: 6602648464, goldin@ocean.ru

GLITKO, Oleg V., ORCID ID: 0009-0005-2313-2326, glitko_kisin@mail.ru

AGLOVA, Yevgeniya A., РИНЦ AuthorID: 1160772, ORCID ID: 0009-0008-6698-0386, Scopus AuthorID: 57396090100, aglova.ea@ocean.ru

GLUKHOVETS, Dmitry I., Cand.Sc. (Phys.-Math.), РИНЦ AuthorID: 924346, ORCID ID: 0000-0001-5641-4227, Scopus AuthorID: 57193736311, glukhovets@ocean.ru

RODIONOV, Maxim A., Cand.Sc. (Phys.-Math.), РИНЦ AuthorID: 203807, ORCID ID: 0000-0002-7397-0548, Scopus AuthorID: 56034199200, maxim_rodionov@mail.ru